Available online at www.sciencedirect.com
SCIENCE DIRECT®
Journal of Molecular Catalysis A: Chemical 220 (2004) 53–65
JOURNAL OF MOLECULAR CATALYSIS A: CHEMICAL
www.elsevier.com/locate/molcata

Effect of chlorine on redox and adsorption characteristics of Mo/Si:Ti catalysts in the oxidative dehydrogenation of ethane

Chang Liu, Umit S. Ozkan*

Department of Chemical Engineering, The Ohio State University, Columbus, OH 43210, USA

Received 23 October 2003; accepted 22 March 2004

Available online 19 July 2004

Abstract

A series of 10%Mo/Si:Ti = 1:1 catalysts modified with chlorine (Cl/Mo = 0.1–2.0) were studied with regard to their activity for the oxidative dehydrogenation of ethane. The effect of chlorine on the redox and adsorption characteristics and, in turn, on the catalytic performance has been investigated. From X-ray diffraction, temperature-programmed reduction and electron spin resonance experiments, it was seen that the addition of chlorine could optimize the redox characteristics of surface molybdena species, i.e. depress the reduction potential of Mo^{6+}, resulting in increased selectivity for ethylene. Temperature-programmed desorption following ethane adsorption showed an increased ease of ethylene desorption from the surface. TPRxn DRIFTS experiments after ethane adsorption, which pointed to a stronger interaction of ethane with the catalyst and increased surface olefinic species suggest that chlorine cannot only affect the further reaction of ethylene over MoO_x catalysts, but also change the interaction of the catalyst with ethane, altering ethane activation steps.

Keywords: Ethane; Ethylene; DRIFTS; ESR; XPS; Molybdenum; Silica-titania

1. Introduction

Although it offers many advantages as compared to steam cracking and direct dehydrogenation, catalytic oxidative dehydrogenation (ODH) of alkanes continues to pose major challenges as a research area [1–5]. Lower alkanes, such as ethane, are inexpensive and readily available for the production of olefins through the ODH process [6]. However, compared to higher alkanes, higher temperatures are required for the activation of ethane and under higher temperatures, ethane and ethylene, the desired product, are easily further oxidized to produce carbon oxides and water. Consequently, maintaining high selectivity towards ethylene while activating ethane effectively is the major challenge for the oxidative dehydrogenation of ethane.

Cavani and Trifiro [2] have grouped the catalysts that are active in the ODH of ethane into two main categories. While Mo- and V-based catalysts have been proven to be active at lower temperatures for the ODH of lower alkanes [7,8], the reaction on these transition metal oxides is heterogeneous and follows the Mars–Van Krevelen mechanism [9], achieving ethylene yields in the range of 15–30% [1,2,8]. Significant increases have also been reported in the ethane ODH activity of catalysts based on Group IA and IIA metals when small quantities of chlorine-containing materials are incorporated either in the feed or directly into catalysts during preparation [10–18]. The reaction occurs through the formation of ethyl radicals that react in the gas-phase to form ethylene. The presence of chlorine is believed to facilitate this desorption-reaction process and the resulting ethylene yield is normally higher compared to those following the Mars–Van Krevelen mechanism at lower temperatures [1,2].

While the positive effects of chlorine to enhance the homogeneous reaction in ethane ODH have been the focus of many studies, the role of chlorine for the surface redox mechanism over easily reducible metal oxide catalysts at lower temperatures is still not well understood [7]. Furthermore, the environmental concerns exclude the use of chlorinated compounds as part of the feed stream. Therefore, chlorine-modified catalysts that can operate at lower temperatures and exhibit sufficient activity and stability can be promising for ODH processes.[1,19].

* Corresponding author. Tel.: +1 614 292 6623; fax: +1 614 292 9615.
E-mail address: ozkan.1@osu.edu (U.S. Ozkan).

1381-1169/$ – see front matter © 2004 Elsevier B.V. All rights reserved.
doi:10.1016/j.molcata.2004.03.049

In our previous work, we have shown Mo/Si:Ti = 1:1 catalysts to be active and selective for the ODH of lower alkanes [20–23]. We have also reported that the addition of small amounts of chlorine to these catalysts can beneficially alter the electronic structure of the surface MoO_x domains and thus the redox mechanism of ethane ODH [24]. In this study, a series of chlorine-modified molybdenum catalysts supported on silica and titania mixed oxides were prepared by a modified sol-gel technique. The catalytic performance of these catalysts was tested for the oxidative dehydrogenation of ethane. Catalysts were characterized by BET surface area measurements, X-ray diffraction (XRD), temperature-programmed reduction (TPR), X-ray photoelectron spectroscopy (XPS), electron spin resonance (ESR), temperature-programmed desorption (TPD) and diffuse reflectance infrared fourier transform spectroscopy (DRIFTS) techniques to elucidate physical–chemical properties of Si:Ti supports, the influence of chlorine on the reducibility of surface molybdena species, adsorption/desorption behavior of reactants and products, and the surface intermediates present during the reaction. These characterization results were correlated with the catalytic reaction performance to achieve a better understanding of the catalytic behavior of chlorine-modified catalysts.

2. Experimental

2.1. Catalyst preparation

Catalysts were prepared by a 'one-pot' sol-gel/co-precipitation technique described previously [25]. For silica-titania mixed-oxide supports, tetraethylorthosilicate (TEOS) (Aldrich) and titanium(IV) isopropoxide (TIPO) (Aldrich) were used as precursors. Ammonium heptamolydate (AHM) (Malinkrodt) was used for molybdenum. The mixture of ethanol and isopropyl alcohol with a 1:1 volume ratio was used as the solvent. Calculated amounts of the silica and titania alkoxide precursors were placed in solvent to yield SiO_2-TiO_2 mixed oxides with a 1:1 molar ratio after calcination. This solution was left stirring, while an aqueous solution containing the necessary amount of AHM for the desired molybdenum loading (10% Mo) was then added dropwise with a syringe pump. The aqueous solution contained the stoichiometric amount of water necessary to hydrolyze all of the alkoxide precursors. For catalysts modified with chlorine, a calculated amount of NH_4Cl (Mallinkrodt) was included in the aqueous solution to give the desired Cl/Mo ratio. The gels formed were stirred for an additional 15 min after all of the aqueous solution had been added and then placed in an oven at 110 °C for overnight drying and solvent removal. After drying, the catalysts were ground into a fine powder and calcined under oxygen at 350 °C for 1 h and 550 °C for 5 h. The synthesized catalysts are listed in Table 1, with Cl/Mo ratios ranging from 0 to 2.

Table 1
Composition and surface area of sol-gel catalysts for the ODH of ethane

Catalyst	Preparation	Surface area (m^2/g)
10%Mo/Si:Ti=1:1	Sol-gel-coprecip.	133
10%(Cl/Mo = 0.1)/Si:Ti = 1:1	Sol-gel-coprecip., NH_4Cl	141
10%(Cl/Mo = 0.3)/Si:Ti = 1:1	Sol-gel-coprecip., NH_4Cl	194
10%(Cl/Mo = 1.0)/Si:Ti = 1:1	Sol-gel-coprecip., NH_4Cl	196
10%(Cl/Mo = 2.0)/Si:Ti = 1:1	Sol-gel-coprecip., NH_4Cl	230

2.2. Catalyst characterization

BET surface area measurements and nitrogen adsorption–desorption isotherms were recorded using a Micromeritics ASAP 2010 instrument. Nitrogen was used as an adsorbent at liquid nitrogen temperature (77 K). The samples were degassed at 200 °C for 8 h before surface area measurements. X-ray diffraction patterns were obtained with a Scintag PAD-V diffractometer with Cu Kα radiation as the X-ray source. The diffractometer was operated at 45 kV and 20 mA and the powder diffraction patterns were recorded in the 2θ range from 20° to 90° with a scan rate of 1°/min.

TPR of catalysts was performed using a laboratory-made gas flow system described in detail elsewhere [26]. Catalyst samples (100 mg) were placed in a 1/4-in.-i.d. quartz U-tube reactor and pre-treated under an oxygen flow at 550 °C for 30 min, and then allowed to cool to room temperature under helium flow. The reduction was performed with 10% hydrogen in argon (30 cm^3/min). The thermal conductivity detector (TCD) was operated in differential mode and the signal transferred to a data acquisition computer. The outlet of the reactor was passed through a column of silica gel to remove moisture formed during the reduction. The temperature program was as follows: 10 min hold at room temperature; 10 °C/min ramp rate to 850 °C and; 10 min hold at 850 °C.

Before XPS analysis, ethane reduction was performed with a Micromeritics ASAP 2010 instrument. For the ethane reduction experiment, a portion of the prepared sample was placed inside a quartz ESR tube (Wilmad) capable of sealing the sample under a gas atmosphere or vacuum. After being recalcined with 800 Torr of oxygen at 550 °C for 30 min and purged to 10^{-3} Torr, the samples were contacted with 500 Torr of ethane at 400 °C for 30 min followed by evacuation at 10^{-3} Torr and backfilled with helium. The samples were then moved to a glove box and transferred to an XPS spectrometer through a controlled-atmosphere transfer chamber. X-ray photoelectron spectroscopy of the catalysts after ethane reduction was performed with a Kratos Ultra Axis spectrometer using Al Kα (1486.3 eV) radiation. Spectra were corrected using the C 1 s signal located at 284.6 eV and the deconvolution was performed using the GRAMS 32 software package.

Electron spin resonance (ESR) spectra were acquired on a Bruker ESP300 electron spin resonance spectrometer. For

ESR spectrum taken under dehydrated conditions, a portion of the prepared samples was recalcined at 550 °C for 30 min under pure oxygen and maintained in the dehydrated state at 110 °C prior to analysis. The spectra were obtained at room temperature with a Klystron frequency of 9.76 GHz at 7.96 mW power and 100 kHz magnetic field modulation. For ethane reduction experiments, the procedure was the same as XPS described above. ESR spectra were recorded under helium atmosphere.

TPD of ethane adsorption was performed using a laboratory-made gas flow system described elsewhere [26]. Catalyst samples (150 mg) were placed in a 1/4-in.-i.d. quartz U-tube reactor, pre-treated under oxygen flow at 550 °C for 30 min, cooled to room temperature under helium flow, and finally flushed with helium for 1 h following 1 h of ethane adsorption. Species desorbing under a helium carrier gas were monitored by a mass spectrometer (HP5890 GC–MS). The GC columns were replaced by an empty capillary column. The mass spectrometer was equipped with a quadrupole mass analyzer that allows tracking of up to 20 mass-to-charge ratios (*m/z*) simultaneously in the selected ion mode. The identification of species with equal *m/z* ratios was accomplished by following characteristic mass fragments of the species. The temperature program was as follows: 10 min hold at room temperature; 10 °C/min ramp rate to 800 °C and; 10 min hold at 800 °C.

DRIFTS of the studied catalysts were performed using a Bruker IFS66 instrument equipped with MCT detectors and a KBr beamsplitter. Catalysts were placed in a sample cup inside a Spectratech diffuse reflectance cell equipped with KBr windows and a thermocouple mount that allowed direct measurement of the surface temperature. Spectra were averaged over 1000 scans in the mid-IR range (400–4000 cm^{-1}) to a nominal 2 cm^{-1} resolution. Prior to collecting spectrum, catalysts were recalcined with 10% oxygen in helium for 30 min at 450 °C surface temperature. For ethane, ethylene and water adsorption experiments, background spectra were taken under helium flow at various temperatures (room temperature, 100, 200, 300, 350, 400, 450 °C). Following background measurements, the adsorption with respective gases was performed for 1 h at room temperature followed by flushing with helium for 1 h at room temperature. Spectra were taken under helium flow at each successive temperature after an equilibration time of 15 min.

2.3. Ethane oxidative dehydrogenation

Cl/Mo catalysts were tested for the ethane ODH reaction in a fixed-bed quartz reactor operating at ambient pressure. Catalyst samples were held in place by a quartz frit. The total flow rate was 25 cc/min with a feed composition of ethane/oxygen/nitrogen = 10/5/85. The major reaction products were ethylene, methane, carbon dioxide, carbon monoxide, and water, which were separated and analyzed online using a HP 5890 series II gas chromatograph containing FID and TCD detectors. Separations were performed using three columns: (1) Hayesep D (8 ft × 1/8 in.) for hydrocarbons and partially oxygenated hydrocarbons; (2) Porapak Q (6 ft × 1/8 in.) and; (3) molecular sieve 5 Å (6 ft × 1/8 in.) for N_2, O_2, CO, CO_2 and H_2O.

In order to study the effectiveness of the catalysts for the ODH of ethane, it is necessary to isolate catalytic activity from gas-phase activity since the contribution from the homogeneous reaction due to ethyl radicals formed at the surface and desorbed into the gas-phase can be significant, especially at higher temperatures. Burch and Grabb have studied homogeneous contributions to the catalytic ODH of ethane and have confirmed that filling the dead space of the reactor with quartz inhibits the gas-phase radical reaction [27]. During catalytic reaction experiments the dead volume of the quartz microreactor was packed with quartz wool and/or ceramic beads to minimize any effects from the homogeneous reaction/surface-initiated gas-phase reaction and to provide a short residence time for ethylene formed. To test the validity of this technique, reaction tests were run using a quartz reactor packed with quartz wool/ceramic beads. The results showed no noticeable conversion of ethane up to 650 °C for the feed conditions studied. The product distributions maintained a carbon balance of 100% (±5%).

3. Results and discussion

3.1. Physical characterization

By comparing the surface area of the prepared catalysts (Table 1), it can be seen that the incorporation of chlorine into Mo/Si:Ti catalysts increases the surface area. Since the active metal and Cl are incorporated into the catalysts during the gelation process, it is possible that the addition of Cl ions affects the formation of the Si:Ti skeleton, leading to significant increases in surface areas.

For the X-ray diffraction patterns obtained on the chlorine-free catalyst (Fig. 1), one broad peak with a center located at a *d*-spacing of 3.59 Å was observed, indicating a finely dispersed anatase titania supported over amorphous silica [28]. All the chlorine-modified catalysts exhibit similar XRD patterns as the Mo-only catalyst, while the anatase diffraction peak becomes just slightly narrower with the addition of chlorine, sugesting an increase in crystallinity of titania in the Si:Ti matrix. Also, no MoO_3 diffraction features were observed for any of the chlorine-modified catalysts indicating that the molybdena species were finely dispersed into the Si:Ti matrix.

3.2. Temperature-programmed reduction

Temperature-programmed reduction experiments were performed on 10%Mo/Si:Ti = 1:1 catalysts with different chlorine loading levels and the results are plotted in Fig. 2. The TPR profiles for all of the catalysts studied are similar, with one major reduction feature in the temperature range

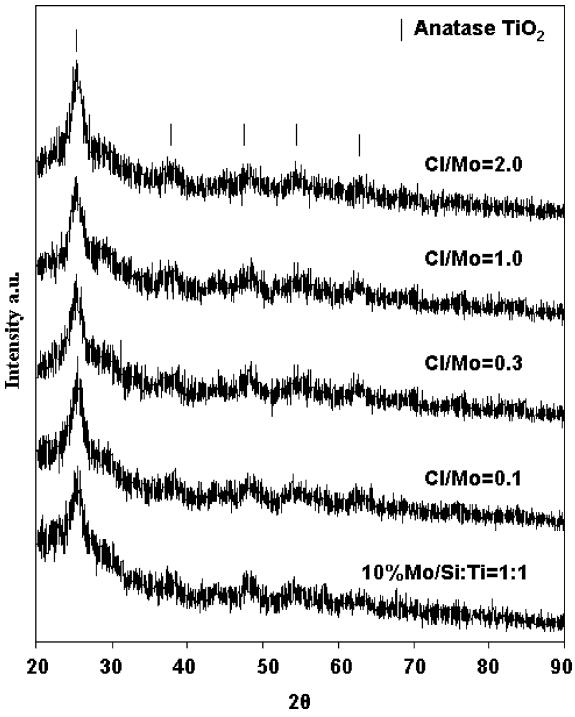

Fig. 1. X-ray diffraction patterns of (Cl/Mo)/Si:Ti catalysts.

from 350 to 500 °C. Since the bare Si:Ti support showed no reduction under the same conditions [24], this feature is assigned to the reduction of supported MoO_x species. The temperature maxima for the reduction features shift to higher temperatures with increasing Cl loading, suggesting a change in the reducibility of the MoO_x species with the incorporation of Cl. Reducibility of the catalyst has significant implications for activation of ethane, which involves a hydrogen abstraction step. For reducible metal oxides operating at lower temperatures such as Mo/Si:Ti catalysts, the hydrogen abstraction involves use of lattice oxygen through the Mars–van Krevelen mechanism. The reducibility of a catalyst with hydrogen can be used to characterize the mobility of lattice oxygen [29,30]. The relative ease of the lattice oxygen removal can also be important in determining the selectivity since further oxidation of the product may also involve lattice oxygen. Therefore, the change in the reducibility of a catalyst by Cl incorporation can have implications for both the activation of ethane and further oxidation of the product, ethylene [31].

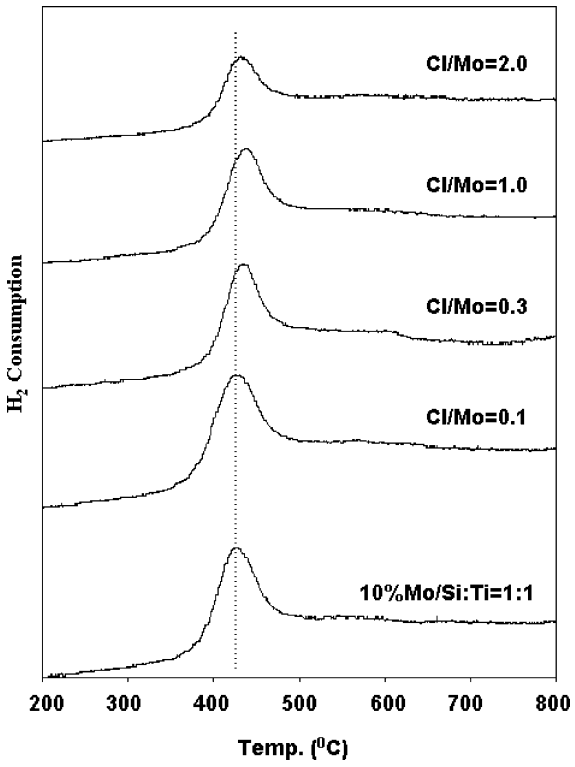

Fig. 2. Temperature-programmed reduction profiles of (Cl/Mo)/Si:Ti catalysts.

3.3. X-ray photoelectron spectroscopy

To further investigate the redox characteristics of the catalysts under reaction conditions and clarify in situ oxidation state changes, X-ray photoelectron spectra were taken of samples that were reduced with ethane. The post- and pre-reduction spectra acquired over the Mo/Si:Ti catalyst are presented in Fig. 3. The Mo 3*d* region of the pre-reduction spectrum exhibited one linked doublet, characteristic of Mo(VI) species in an oxide matrix. The spectrum taken following ethane reduction, on the other hand, showed the co-existence of the Mo(VI)/Mo(V) oxidation states, corresponding to Mo $3d_{5/2}$ and $3d_{3/2}$ binding energy values at 235.9/234.7 and 232.7/231.4 eV, respectively [32–34]. The deconvolution results are presented in the figure. No Mo(IV) was detected after ethane reduction. Since under reaction conditions, where the gas-phase contains oxygen, further reduction to Mo(IV) is even less likely, it can be concluded that a redox cycle between Mo (VI)/Mo(V) is the dominant mechanism.

3.4. Electron spin resonance

ESR techniques have been widely used to investigate the surface chemistry of metal oxide catalysts [35]. In molybdena catalysts, where the vast majority of Mo ions are in Mo(VI) oxidation state, calcination at high temperatures as well as reduction under reaction conditions can lead to the formation of paramagnetic Mo(V) centers [36], which are ESR sensitive and can be used to gain insight into the coordination environment of the surface molybdena species.

In this study, ESR spectra were recorded on ambient-exposed and dehydrated Cl/Mo catalysts at room temperature (Figs. 4 and 5). Different from our previous study on K/Mo catalysts [22], where a noticeable broadening of the Mo(V) signal appears upon dehydration without substantial loss of intensity, here both the ambient and dehydrated spectra are characteristic of Mo(V) in a state of nonaxial symmetry, indicating the adsorption of atmospheric water does not

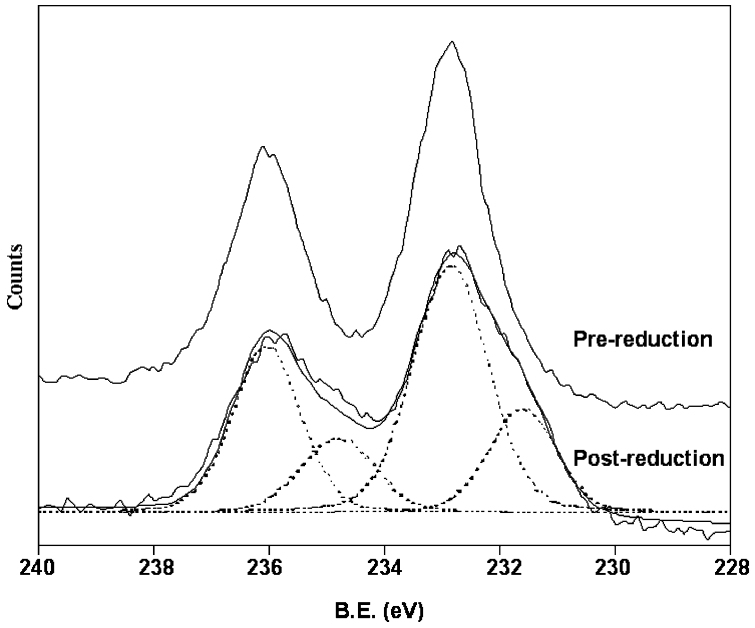

Fig. 3. Pre- and post-ethane reduction X-ray photoelectron spectra of 10%Mo/Si:Ti = 1:1.

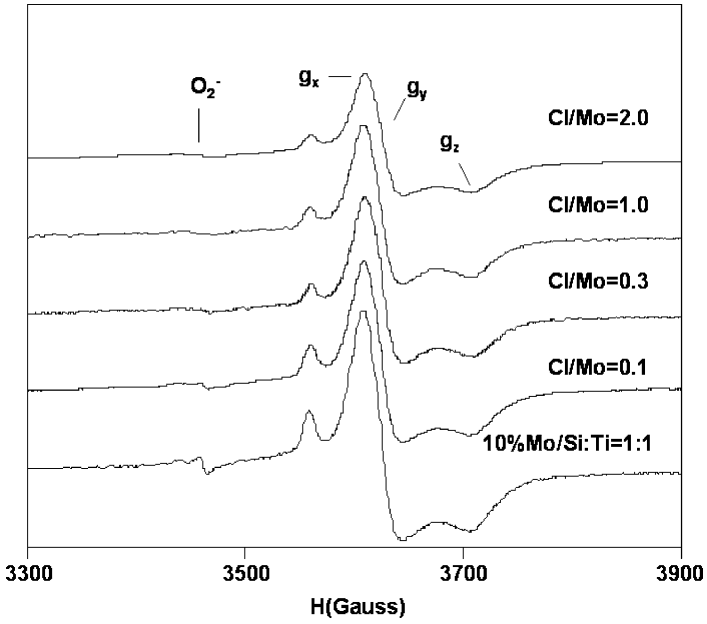

Fig. 4. ESR spectra of (Cl/Mo)/Si:Ti catalysts under ambient conditions.

have a strong effect on the dispersion and coordination of MoO_x domains. Parallel and perpendicular parameter values are defined as $g_T = (g_x + g_y)/2$ and $g_{II} = g_z$, and the g_T and g_{II} values of Mo(V) obtained from ambient and dehydrated Cl/Mo samples are presented in Table 2. Compared with the g values for hexa-coordinated Mo(V) species reported in the literature (Table 3) [37–39], it can be seen that with the addition of chlorine there is no change in the coordination sphere of Mo(V), i.e. both Mo-only and Cl-doped catalysts showed Mo(V) in a hexa-coordination environment.

Another feature evident in both the ambient and dehydrated ESR spectra is the signal from the superoxide ion

Table 2
The g-tensor of Mo(V) in (Cl/Mo)/Si:Ti catalysts

Catalyst	Ambient		Dehydrated	
	g_T	g_{II}	g_T	g_{II}
10%Mo/Si:Ti = 1:1	1.942	1.89	1.942	1.893
Cl/Mo = 0.1	1.941	1.893	1.94	1.893
Cl/Mo = 0.3	1.94	1.894	1.94	1.892
Cl/Mo = 1.0	1.94	1.893	1.94	1.893
Cl/Mo = 2.0	1.939	1.893	1.942	1.895

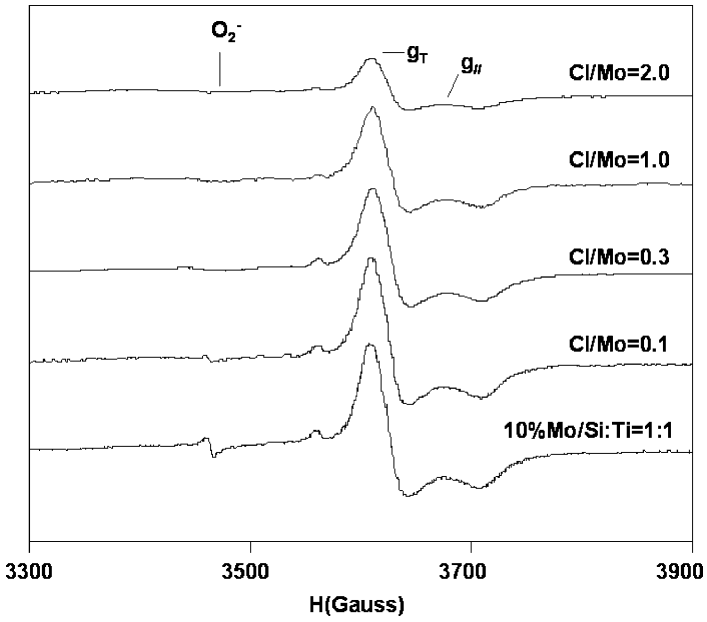

Fig. 5. ESR spectra of (Cl/Mo)/Si:Ti catalysts under dehydrated conditions.

(O_2^-) with a characteristic average g value of 2.011 [40]. It is interesting to note that this signal becomes smaller with the addition of chlorine and almost disappears at higher Cl/Mo ratios. O_2^- can be formed upon interaction of molecular oxygen with surface anionic vacancies [41]. During ethane ODH these superoxide species as well as other activated oxygen species can be inserted into ethane in a non-selective manner through electrophillic addition and contribute to total combustion [29,30,42]. The source of the superoxide ion cannot be determined since these species can exist and be stabilized both in crystalline TiO_2 [40] and in silica domains [35], and can also be associated with the formation of Mo(V) species. However, the change in intensity could be a further indication that, with chlorine addition, the mobility and activity of lattice oxygen at the catalyst surface is suppressed, in agreement with the TPR results.

The variation of integral intensity for Mo(V) species with Cl loading for dehydrated and ambient samples is shown in Fig. 6. Compared with catalysts at ambient conditions, the intensities are lower for the dehydrated samples since they are likely to reoxidize during the calcination/dehydration process. The intensity of Mo(V) species decreases with Cl loading in both cases. This could be the result of a less reducible catalyst surface, leading to the formation of fewer Mo(V) centers during the calcination process.

To further investigate the effect of chlorine on the interaction of ethane with the catalyst surface, ESR spectra were taken of samples that were reduced in ethane. The pre- and post-reduction spectra of Cl-free and Cl-containing samples are shown in Fig. 7. It can be seen that after reduction with ethane, there is a broadening of the ESR line widths and spectra become quasi-axial. The perpendicular and parallel values of the g-tensor and integral intensity of Mo(V) species for post-reduction samples are given in Table 4. The Cl-free sample shows a much higher intensity for Mo(V) compared to the Cl-containing catalysts. When the g values obtained from the post-reduction samples are compared to those reported in the literature (Table 5) [35,43–45], one can see that the coordination of Mo(V) species change from a hexa-coordination to a hepta-coordination environment.

Table 4
The g-tensor values and intensity of Mo(V) species after ethane reduction

Catalyst	Intensity	g_T	g_{II}
10%Mo/Si:Ti = 1:1	1447	1.956	1.899
Cl/Mo = 1.0	909.7	1.956	1.898

Table 3
The g-tensor values of hexa-coordinated Mo(V) species from literature [37–39]

Catalyst	g_T	g_{II}
$MoOx/SiO_2$	1.944	1.890
MoO_3/ZnO	1.942	1.870
Mo/H-ZSM-5	1.943	1.882

Table 5
The g-tensor values of hexa-, hepta- and tetra-coordinated Mo(V) species from literature [35,43–45]

Coordination	g_T	g_{II}
Mo(V)6c	1.944	1.892
Mo(V)5c	1.957	1.866
Mo(V)4c	1.926	1.755

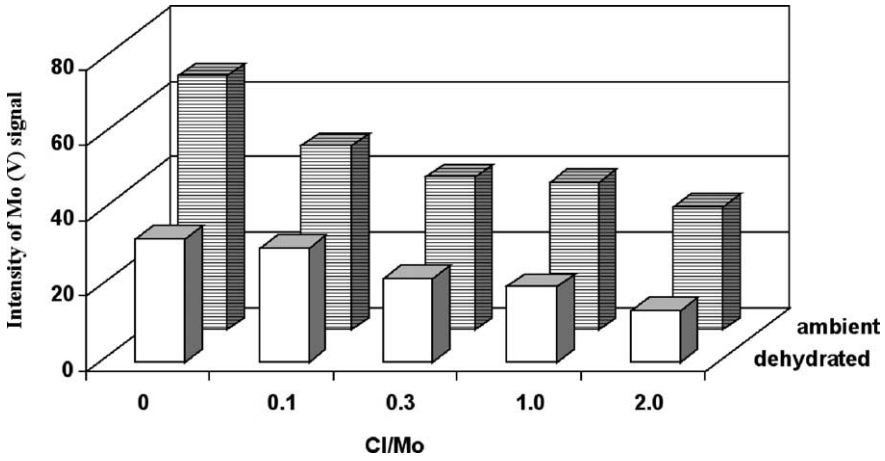

Fig. 6. Integrated intensities of Mo(V) species for (Cl/Mo)/Si:Ti catalysts under ambient and dehydrated conditions.

Since there is a substantial increase in the integral intensity of Mo(V) after ethane reduction, we may conclude that the major contribution of this shift is due to the reduction of Mo(VI) species to penta-coordinated Mo(V) species rather than the coordination change of the existing Mo(V) species. When comparing the post-reduction Mo-only and Cl-doped catalysts, it can be seen that the intensity is much lower on the Cl/Mo catalyst. Since our XPS results showed no Mo(IV) species on the surface of catalysts reduced with ethane, suggesting that Mo(VI) species do not further reduce to Mo(IV), the intensity of Mo(V) species obtained by ESR following ethane reduction can be taken as a measure of the reducibility of MoO_x on the surface. Once again, the incorporation of chlorine appears to lead to less reducible molybdena species on the surface.

3.5. Temperature-programmed desorption

Analysis of the desorbed species after ethane adsorption showed ethane, ethylene, water, methane, carbon dioxide, carbon monoxide, and trace amounts of acetaldehyde desorbing from the surface. Ethylene desorption profiles for 10%Mo/Si:Ti = 1:1 and chlorine-containing catalysts of Cl/Mo = 0.3 and 1.0 are plotted in Fig. 8a. Although ethane creates the same fragmented species as ethylene in the mass spectrometer, by following fragments created by both, we determined that the first desorption features (<150 °C) are associated with ethane desorption and the remainder of the profile belongs to ethylene alone. An important aspect of these profiles is that the major desorption feature shifts to lower temperature with increasing chlorine loading, which

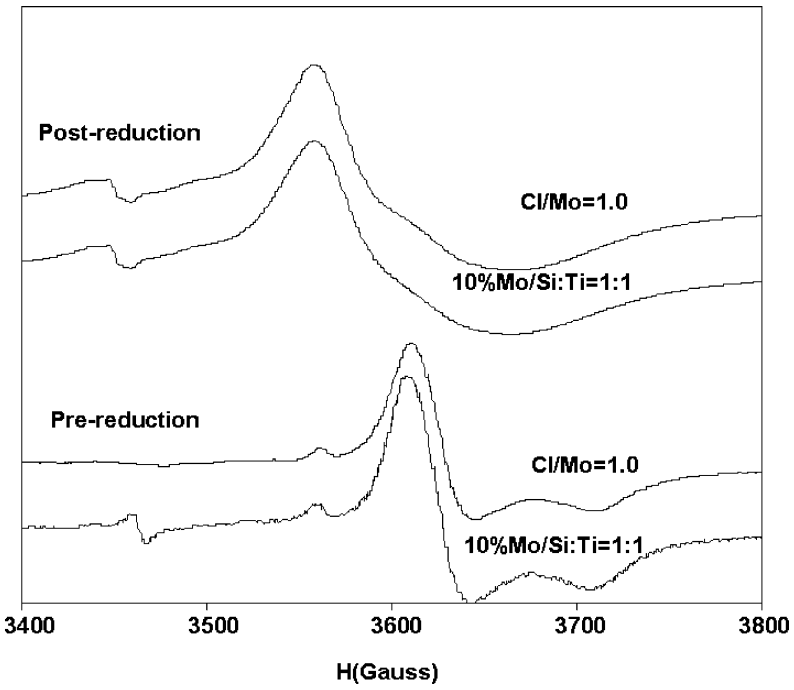

Fig. 7. Pre- and post-reduction ESR spectra of Cl-free and Cl-containing catalysts.

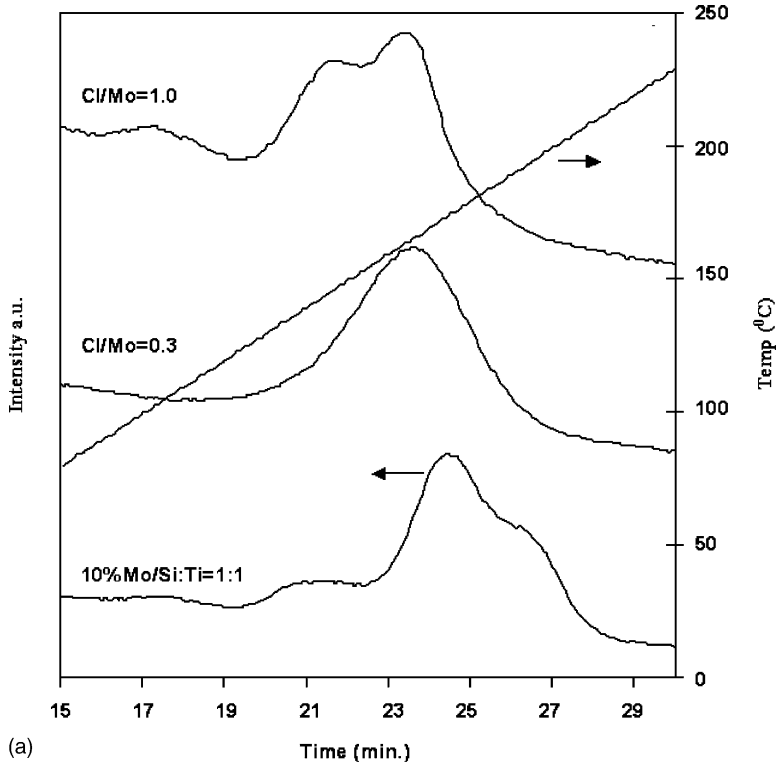

(a)

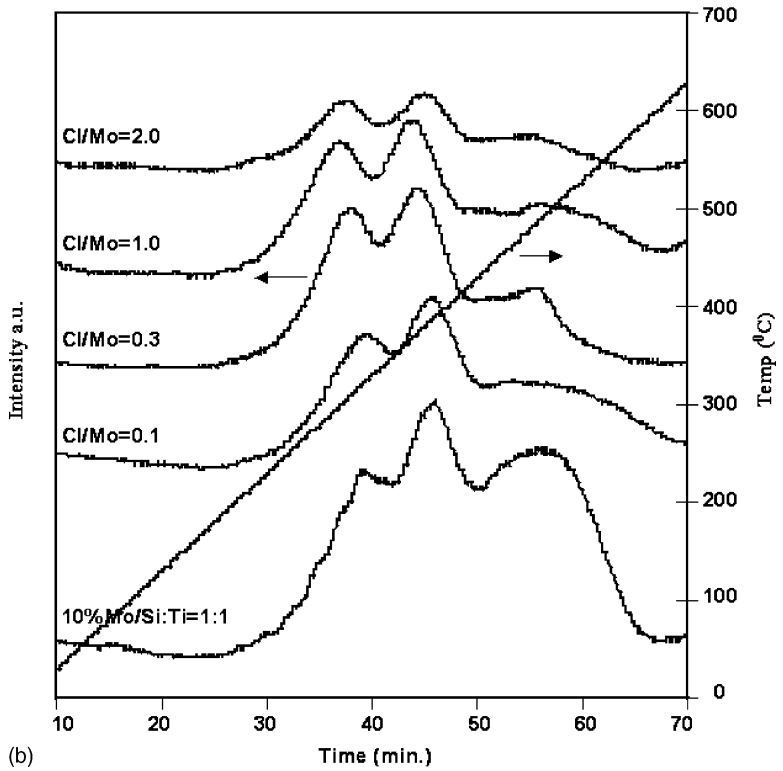

(b)

Fig. 8. Temperature-programmed desorption profiles following ethane adsorption: (a) ethylene desorption profile; (b) CO_2 desorption profile.

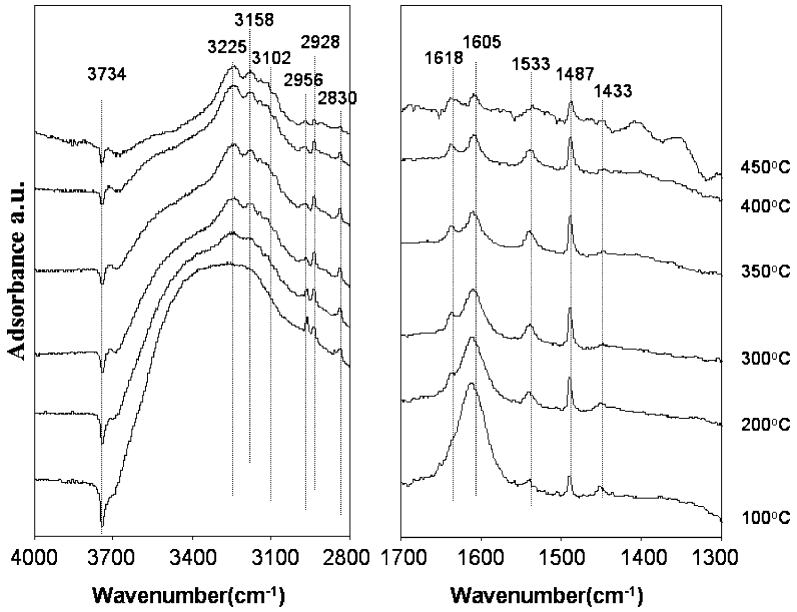

Fig. 9. In situ DRIFT spectra taken during ethane TPD for chlorine-containing catalyst.

points to an ease of ethylene desorption from the surface for the chlorine-containing catalysts. At the same time, the amount of ethylene desorption is seen to be directly related to Cl content as the major desorption feature increases in intensity with Cl loading. The desorption profiles for carbon dioxide are plotted in Fig. 8b. There are three significant desorption features present on the Mo-only catalyst around 300, 400, and 500 °C. With the addition of chlorine, these desorption features appear to be suppressed and present a broader profile. While TPD results cannot be directly related to the behavior under reaction conditions, both the ethylene and carbon dioxide desorption profiles indicate that the addition of chlorine appears to inhibit CO_2 formation, leading to increased ethylene selectivity.

3.6. In situ DRIFTS/temperature-programmed desorption

To further investigate the interaction of ethane with Cl/Mo catalysts and ascertain the different surface intermediates present during reaction, in situ DRIFTS experiments were performed during temperature-programmed desorption after ethane, ethylene and water adsorption over the catalysts with Cl/Mo molar ratios of 0 and 0.1 and the results are presented in Figs. 9–11.

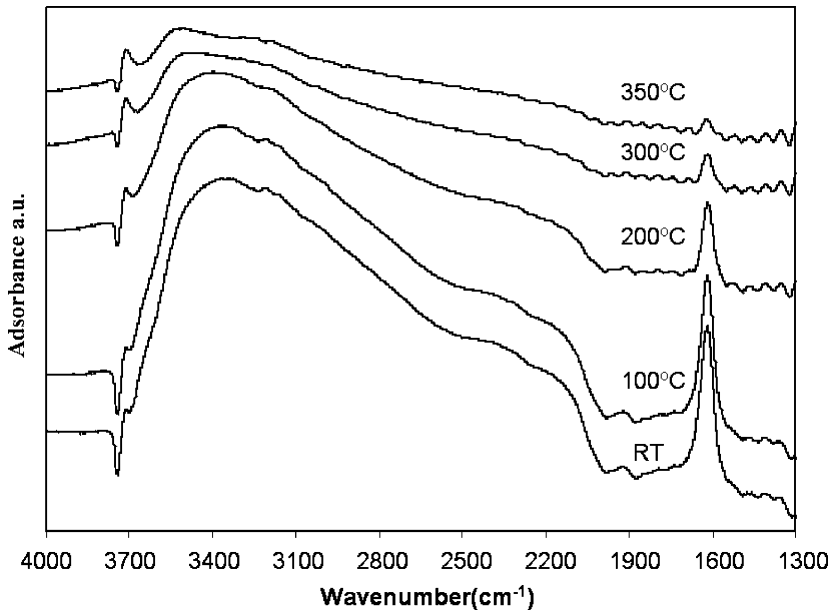

Fig. 10. In situ DRIFT spectra taken during water TPD for chlorine-containing catalyst.

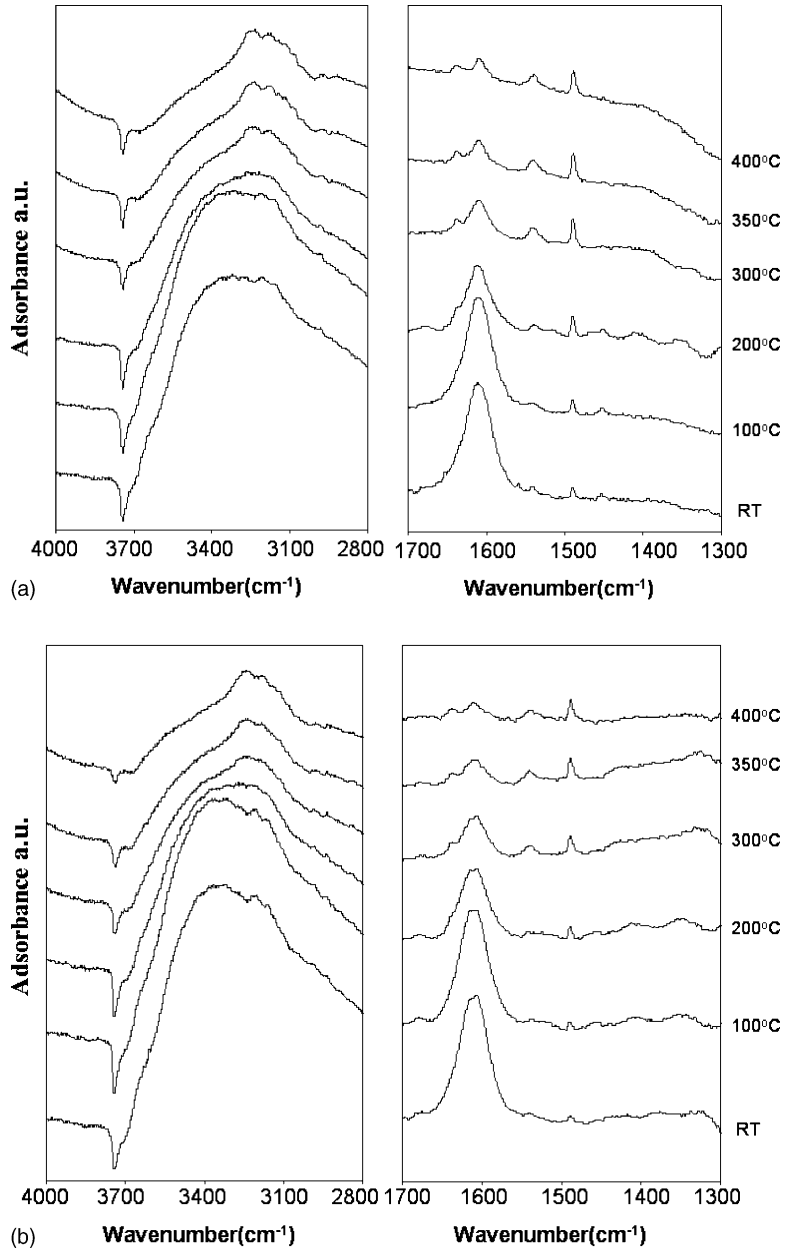

Fig. 11. In situ DRIFT spectra taken during ethylene TPD: (a) chlorine-free catalyst; (b) chlorine-containing catalyst.

Spectra taken at different temperatures after the chamber was flushed with helium are shown in Fig. 9. The negative peaks seen at 3734 cm^{-1} correspond to OH groups which are present on the surface prior to adsorption, but they disappear through interaction with adsorbing ethane molecules. There are multiple bands at 3225, 3158, 3102 cm^{-1}, which could be partly due to the OH stretchings of hydrogen bonded adsorbed species formed from the interaction of ethane with the catalyst surface [47]. The bands located at 2956, 2928 and 2830 cm^{-1} can be assigned to surface ethyl species from the dissociative chemisorption of ethane [46–48]. These surface ethyl species appear to form readily even at room temperature (not shown), but decrease gradually in intensity at higher temperatures. In the typical carbon–oxygen vibration frequency range (1900–1300 cm^{-1}), there are bands located at 1618 and weak bands at 1380 and 1341 cm^{-1}, which are likely to be due to C=C, COH and C–O stretching vibrations of an enolate-type species, respectively [49,50]. As reported previously [51,52], this species could be a precursor to aldehyde, as seen through the 1487 and weak 1314 cm^{-1} bands. The 1605 and 1433 cm^{-1} bands observed at higher temperatures are likely due to acetate species, while 1533 and weak 1380 cm^{-1} bands can be associated with formate ions [51–54], both of which are generally recognized as the most likely precursors for CO_x formation. A similar experiment performed over Mo-only catalyst gave rise to very similar spectral features with small differences in relative intensities (not shown).

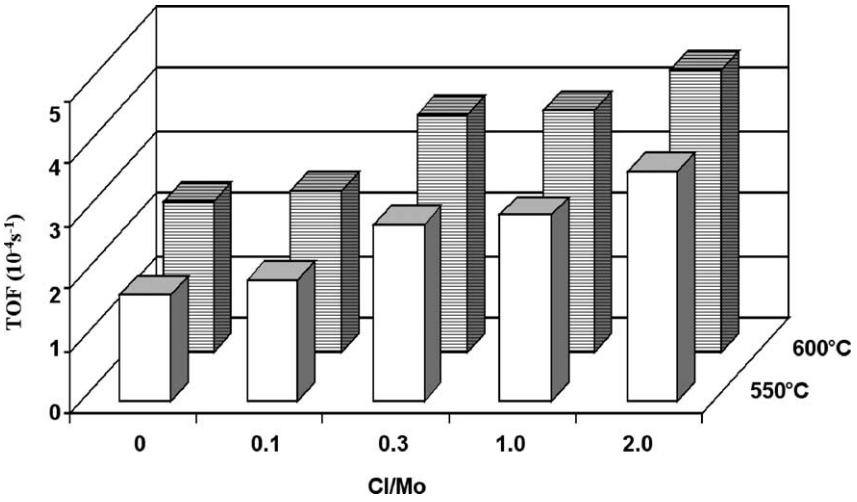

Fig. 12. Ethylene formation TOFs for (Cl/Mo)/Si:Ti catalysts.

A very prominent feature seen at lower temperatures in Fig. 9 is the band at 1605 cm^{-1}, which is coupled with a very broad band in the 3300–3600 cm^{-1} range. These features are due to adsorbed water [47]. The intensities of both bands decrease simultaneously with increasing temperature. To verify this assignment, a similar experiment was performed where only water was adsorbed at room temperature and spectra were taken at different temperatures after the system was flushed with helium at room temperature (Fig. 10). Similar features were observed following water adsorption, verifying that the bands seen in Fig. 9 were due to water formed from adsorbed ethane.

The DRIFTS spectra taken over Mo-only and Cl-doped catalysts after ethylene adsorption are compared in Fig. 11. One interesting difference from ethane adsorption is that the multiple bands between 3300 and 2800 cm^{-1} are much weaker on both catalysts and even less pronounced on chlorine-doped catalyst, indicating weaker interaction of ethylene with the catalyst surface after chlorine addition. This observation is consistent with the easier desorption of ethylene from chlorine-doped catalysts seen in TPD experiments. Furthermore, over the chlorine-modified catalyst, the bands from acetate and formate species only appear at higher temperatures and are less pronounced. These differences in the carbon–oxygen region of the DRIFT spectra indicate that different, and perhaps unselective mechanistic steps take place on the Mo-only catalyst after ethylene adsorption, and they are suppressed by the addition of chlorine. The bands that correspond to water are observed following ethylene adsorption also, resulting in poorer resolution in

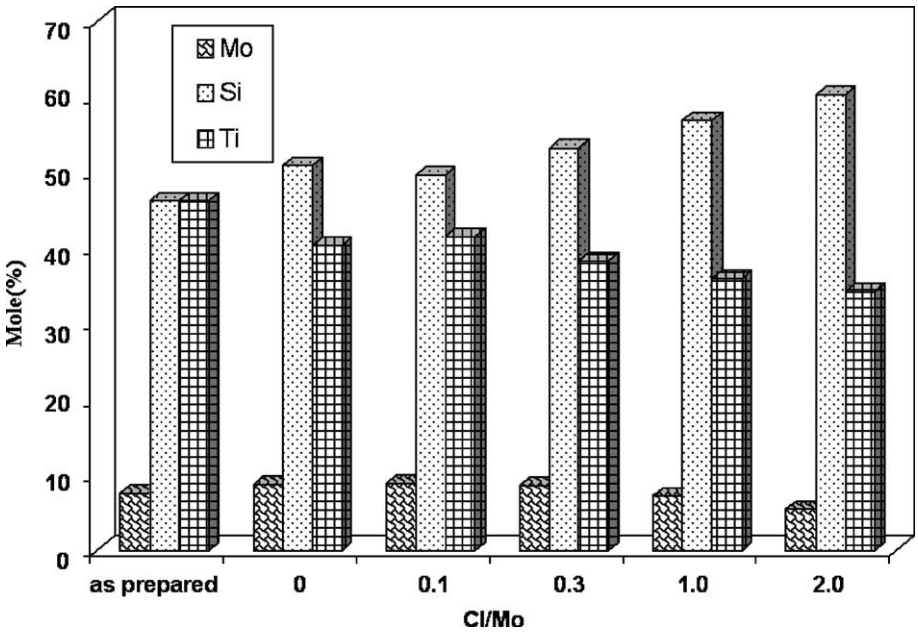

Fig. 13. Surface concentrations of Mo, Si, and Ti of (Cl/Mo)/Si:Ti catalysts calculated from XPS analysis.

Table 6
Ethane ODH data for (Cl/Mo)/Si:Ti catalysts

Catalyst	C_2H_6 conversion (%)		C_2H_4 selectivity (%)		C_2H_4 yield (%)	
	550 °C	600 °C	550 °C	600 °C	550 °C	600 °C
10%Mo/Si:Ti = 1:1	23.5	31.1	30.2	32.6	7.1	10.1
Cl/Mo = 0.1	22.5	30.1	34.1	34.4	7.6	10.3
Cl/Mo = 0.3	23.2	29	34.7	37.8	8.1	11
Cl/Mo = 1.0	25.8	31	33.2	36.2	8.6	11.2
Cl/Mo = 2.0	24.8	28.3	35.8	38.6	8.9	10.9

the 3300 and 2800 cm^{-1} wavenumber range and complicating the band assignment in the carbon–oxygen range. The negative bands corresponding to OH groups are also observed following ethylene adsorption. It is conceivable that surface OH groups may act as 'anchors' for the hydrocarbon molecules and may play a role in the formation of formate and acetate surface species [55].

3.7. Ethane oxidative dehydrogenation

Catalysts with Cl/Mo ratios ranging from 0 to 2 were tested for the ethane ODH reaction using 100 m^2 of equal surface area in the reactor and at temperatures of 550 and 600 °C. The feed percentages for these experiments were ethane/oxygen/nitrogen=10/5/85. Oxygen conversion was nearly 100% for all runs. Reaction data were taken after steady-state was reached. Ethane conversion as well as ethylene selectivity and yield data are presented in Table 6.

Compared with the Mo-only catalyst, there is not a noticeable increase in the activity of chlorine-containing catalysts. In fact, at 600°C, the ethane conversion is lower for all Cl-containing catalysts. The selectivity and yield for ethylene, on the other hand, are higher for the Cl-containing catalyst at both temperatures. When reaction data are presented in the form of TOF for ethylene formation, the difference is more noticeable (Fig. 12). Since the catalysts are prepared by a sol-gel technique and not all Mo is on the surface, the absolute values of TOFs may not represent the true turn-over-frequencies. Also, the differences in surface areas may make a comparison based on TOF more difficult. However, when we examine the surface concentrations of the three metal atoms using XPS (Fig. 13), we see that the concentration of Mo is constant for most of the catalysts, with a small decrease at higher Cl loadings. This observation would imply that if we were to quantify the surface Mo atoms and normalize the reaction data with respect to Mo species that are on the surface, the trend we observe in Fig. 12 would not only still hold, but also become more pronounced.

4. Conclusions

When the reaction results are viewed in light of the characterization experiments, one sees that the role of Cl on ethylene yield may be two-fold. On one hand, the Cl addition appears to inhibit further reaction of ethylene, by making the ethylene adsorption weaker and allowing it to escape to the gas-phase more easily, as seen in TPD and DRIFTS experiments. On the other hand, it also seems that Cl addition suppresses the oxidation potential of the catalyst. TPR, XPS and ESR results showed a decreased redox potential of Mo(VI) and lower mobility of lattice oxygen with chlorine addition, which might account for a 'balance' effect on ethane ODH, in which a less reducible catalyst may cause the total activation of ethane to be suppressed, but the unselective oxidation could also be hindered since a too labile oxygen species could lead to total oxidation. While the promotion effects of chlorine addition have been characterized in terms of the reactivity of formed ethylene, it is conceivable that this alone is not sufficient to explain the difference in the catalytic performance. It is quite likely that the addition of chlorine not only affects the reactivity of ethylene by making it easier to desorb into the gas-phase, but also affects the intermediate steps following ethane activation. The DRIFTS results over the Cl-containing catalysts which show stronger features of surface ethyl species and weaker bands from formate and acetate species, which are known to be the primary precursors for carbon oxides, support this assertion.

Acknowledgements

Financial support provided by National Science Foundation (Grant CTS-9412544) is gratefully acknowledged. The authors also thank Dr. Rick, B. Watson and Dr. Xueqin Wang for their technical assistance at the early stages of the project.

References

[1] H.H. Kung, Adv. Catal. 40 (1994) 1.
[2] F. Cavani, F. Trifiro, Catal. Today 24 (1995) 307.
[3] E.A. Mamedov, V. Cortes-Corberan, Appl. Catal. 127 (1995) 1.
[4] Council for Chemical Research, US DOE, Catalyst Technology Roadmap Report: Build Upon Technology Vision 2020, The US Chemical Industry, ACS workshop, Washington, DC, USA, 1997.
[5] M. Baerns, O. Buyevskaya, Catal Today 45 (1998) 13.
[6] F. Cavani, M. Koutyrev, F. Trifiro, Catal. Today 28 (1996) 319.

[7] M.A. Banares, Catal. Today 51 (1999) 319.
[8] E.M. Thornsteinson, T.P. Wilson, F.G. Yound, P.H. Kasai, J. Catal. 52 (1978) 116.
[9] B.K. Hodnet, Heterogeneous Catalytic Oxidation, Wiley, New York, 2000.
[10] R. Burch, S.C. Tsang, Appl. Catal. 65 (1990) 259.
[11] D. Wang, M.P. Roybek, J.H. Lunsford, J. Catal. 151 (1995) 155.
[12] S. Sugiyama, N. Kondo, K. Satomi, H. Hayashi, J.B. Moffat, J. Mol. Catal. 95 (1995) 35.
[13] S.S. Hong, J.B. Moffat, Catal. Lett. 40 (1996) 1.
[14] W. Ueda, S.W. Lin, I. Tohmoto, Catal. Lett. 44 (1997) 241.
[15] Q. Ge, B. Zhao, C. Yu, W. Li, H. Xu, Catal. Lett. 68 (2000) 59.
[16] S. Wang, K. Murata, T. Hayakawa, S. Hamakawa, K. Suzuki, Eng. Fue. 14 (2000) 899.
[17] H.X. Dai, C.T. Au, Y. Chan, K.C. Hui, Y.L. Leung, Appl. Catal. 213 (2001) 91.
[18] S. Fuchs, L. Leveles, K. Seshan, L. Lefferts, A. Lemonidou, J.A. Lercher, Top. Catal. 15 (2001) 169.
[19] G. Grubert, E. Kondratenko, S. Kolf, M. Baerns, P. Geem, R. Parton, Catal. Today 81 (2003) 337.
[20] R.B. Watson, U.S. Ozkan, J. Catal. 191 (2000) 12.
[21] R.B. Watson, U.S. Ozkan, J. Catal. 208 (2002) 124.
[22] R.B. Watson, U.S. Ozkan, J. Phys. Chem. 106 (2002) 6930.
[23] R.B. Watson, U.S. Ozkan, J. Mol. Catal. 194 (2003) 115.
[24] R.B. Watson, U.S. Ozkan, J. Mol. Catal. 208 (2004) 233.
[25] US Patent no. 6,521,808 (2003).
[26] U.S. Ozkan, Y. Cai, M.W. Kumthekar, L. Zhang, J. Catal. 142 (1993) 182.
[27] R. Burch, E.M. Crabb, Appl. Catal. 97 (1993) 49.
[28] H. Izutsu, P.K. Nair, K. Maeda, Y. Kiyozumi, Mizukami, F. Mater. Res. Bull. 32 (1997) 1303.
[29] E.N. Voskeresenkaya, V.G. Roguleva, A.G. Anshits, Catal. Rev. Sci. Eng. 37 (1995) 101.
[30] Y. Ng Lee, F. Sapina, E. Martinez, J.V. Folgado, V. Cortes Corgeran, in: R.K. Grasselli, S.T. Oyama, A.M. Gaffney, J.E. Lyons (Eds.), Stud. Surf. Sci. Catal. 110 (1997) 747.
[31] R. Schlogl, A. Knop-Gericke, M. Havecker, U. Wild, D. Frickel, T. Ressler, R.E. Jentoft, J. Wienhold, G. Mestl, A. Blume, O. Timpe, Y. Uchida, Top. Catal. 15 (2001) 219.
[32] M. Orita, I. Kojima, E. Iyazaki, Bull. Chem. Soc. Jpn. 59 (1986) 689.
[33] L. Portela, P. Grange, B. Delmon, J. Catal. 156 (1995) 243.
[34] M. Nagai, Y. Goto, H. Ishii, S. Omi, Appl. Catal. 192 (2000) 189.
[35] Z. Sojka, M. Che, Surf. Chem. Catal. 3 (2000) 163.
[36] L.E. Cadus, M.C. Abello, M.F. Gomez, J.B. Rivarola, Ind. Eng. Chem. Res. 35 (1996) 14.
[37] Z. Sojka, M. Che, J. Phys. Chem. 100 (1996) 14776.
[38] K. Nakamura, K. Eda, S. Hasegawa, N. Sotani, Appl. Catal. A 178 (1999) 167.
[39] S. Li, C. Zhang, Q. Kan, D. Wang, T. Wu, L. Lin, Appl. Catal. A 187 (1999) 199.
[40] Q. Zhao, X. Bao, Y. Wang, L. Lin, G. Li, X. Guo, X. Wang, J. Mol. Catal. 157 (2000) 265.
[41] R.Q. Long, Y.P. Huang, H.L. Wan, J. Raman Spectrosc. 28 (1997) 29.
[42] V.D. Sokolovskii, Catal. Rev. Sci. Eng. 32 (1990) 1.
[43] Z. Sojka, A. Adamski, M. Che, J. Mol. Catal. 112 (1996) 469.
[44] C. Louis, M. Che, M. Anpo, J. Catal. 141 (1993) 453.
[45] M. Che, Z. Sojka, Top. Catal. 15 (2001) 2.
[46] J. Pacansky, B. Schrader, J. Phys. Chem. 78 (1983) 1033.
[47] G. Karamullaoglu, S. Onen, T. Dogu, Chem. Eng. Proc. 41 (2002) 337.
[48] C. Cruz, N. Sheppard, Phys. Chem. Chem. Phys. 1 (1999) 329.
[49] E.W. Thornton, P.G. Harrison, J. Chem. Soc., Faraday Trans. 1 71 (1975) 2468.
[50] P.G. Harrison, B. Maunders, J. Chem. Soc., Faraday Trans. 1 81 (1985) 1311.
[51] G. Busca, E. Finocchio, V. Lorenzelli, G. Ramis, M. Baldi, Catal. Today 49 (1999) 453.
[52] E. Finocchio, G. Busca, V. Lorenzelli, R.J. Willey, J. Catal. 151 (1995) 204.
[53] A.A. Davydov, A.A. Budneva, V.D. Sokolovskii, Kinet. Katal. 22 (1981) 213.
[54] V.A. Matyshak, O.V. Krylov, Catal. Today 25 (1995) 1.
[55] S. Trautmann, M. Baerns, J. Catal. 136 (1992) 613.